Proc. Indian natn. Sci. Acad., **60**, A, No. 1, 1994, pp. 369-385.

STUDIES ON ATMOSPHERIC AEROSOLS AT A COASTAL STATION, TRIVANDRUM

B V KRISHNA MURTHY
Space Physics Laboratory, Vikram Sarabhai Space Centre, Trivandrum-695 022, *India*

(*Received* 3 *June* 1993; *Accepted* 5 *July* 1993)

Studies on atmospheric aerosols are being carried out at the tropical coastal station, Trivandrum (8°33'N, 77°E). These are based on the observations by Laser radar and Multiwavelength Radiometer. In this paper, some of the major scientific results obtained from these studies are presented.

Key Words: Atmospheric Aerosols; Aerosol Extinction; Tropical Region

Introduction

Atmospheric aerosols are defined as particles in liquid or solid phase suspended in the atmosphere. These particles cover a wide range of sizes extending from about 10^{-9} m to 10^{-4} m. Aerosols play an important role in the radiation budget of the earth-atmosphere system, atmospheric chemistry and atmospheric electrical conductivity.

Aerosols scatter and absorb electromagnetic radiation from the sun and the earth depending on their size distribution, composition (determining the refractive index) and wavelength of the radiation. The relative amount of absorption and scatter is governed by the aerosol single scattering albedo (w_0), the scattering asymmetry factor (g), the optical depth (τ) and the albedo of the underlying surface. If the aerosols are weakly absorbing type ($w_0 \approx 1$), they predominantly scatter the radiation, increasing the amount of solar radiation backscattered to space. This reduces the energy input to the earth-atmosphere system. The magnitude of this increase in planetary albedo is a function of aerosol size distribution and total optical depth. The asymmetry factor 'g' at a given wavelength increases with increasing particle size for a fixed aerosol composition. This means, that smaller particles tend to increase the planetary albedo in comparison with the large particles for the same optical depth. Absorbing aerosols ($w_0 < 1$) tend to reduce the solar energy lost from the earth-atmosphere system by absorbing the solar radiation. Therefore, this tends to increase the energy input to the earth-atmosphere system.

At infrared wavelengths, since the aerosol particle sizes are, in general, smaller than the wavelength and also since most materials exhibit absorption at these wavelengths, the single scattering albedo tends to be small. Thus, aerosols can be treated mainly as absorbers at infrared wavelengths. It follows that the main effect of aerosols at infrared wavelengths is to increase the total emissivity of the atmospheric layer in which they reside.

The radiative effects of aerosols, especially with regard to aerosol inputs due to major volcanic eruptions, have been studied by a number of workers[1,2,3,4,5]. Following the eruption of El Chichon volcano in 1982, a warming of the stratosphere by about a few degrees K was predicted and observations supported this prediction[4]. A similar warming of stratosphere has also been observed following the eruption of Mt. Pinatubo Volcano[5] in 1991. The model prediction for surface temperatures (for El Chichon and Mt. Pinatubo eruptions) are in the range of -0.5 °K (cooling) and so far there appeares to be nc unambiguous observational evidence linking surface temperature changes with these volcanic eruptions[6].

The presence of aerosols in the atmosphere can support heterogeneous chemistry depending upon the atmospheric species taking part. Heterogeneous chemistry involves chemical reactions occurring on particle surfaces and in aqueous solutions. In recent years, the role of heterogeneous chemistry has come to be recognized as very important and crucial in the Antarctic ozone hole phenomenon. Reactions involving polar stratospheric cloud ice particle surfaces in the chlorine chemistry are generally believed to offer explanation for the Antarctic ozone hole phenomenon.

The role of aerosols in electrical conductivity of the stratosphere has been well recognized. Ions can act as nucleation centres to form aerosols and aerosols, in turn, can affect the ionization through heterogeneous chemistry. The presence of aerosols leads to decrease in electrical mobility and hence, in corresponding decrease in conductivity.

In view of the importance of aerosols in atmospheric processes as briefly outlined above, an understanding of the physical characteristics of atmospheric aerosols and their spatial and temporal variations is essential. While there is considerable information on stratospheric aerosols, information on tropospheric aerosols is rather scanty, especially at tropical latitudes. A programme of research on Atmospheric aerosols was started in the Space Physics Laboratory, Trivandrum in the early eighties and it is a continuing programme of the Laboratory. Some of the main scientific results obtained from this programme are presented in the following.

Ruby Laser Radar

Using a high power pulsed Ruby laser radar (Ruby Lidar), studies on tropospheric and stratospheric aerosols have been carried out at Trivandrum. Lidars essentially provide altitude resolved information on aerosol extinction/backscatter coefficients. The ruby lidar at Trivandrum consists of a ruby laser transmitter at 694.3 nm wavelength with a pulse energy of ~1J in a pulse width of ~4μs. The laser beam is directed vertically up into the atmosphere. The backscattered laser signal by atmospheric molecules and aerosols is received using a cassegrain type telescope consisting of a 12″ parabolic primary mirror and a 4″ hyperbolic secondary mirror. The received scattered signal is collimated using a suitable optical system and is passed through an interference filter whose centre wavelength of transmission is 694.3nm. The filtered signal is detected using a cooled photomultiplier and the detected signal is processed and recorded for analysis.

The backscatter signal power $p(h_1)$ from a height interval $\Delta h(=c\ \Delta t/2)$ centred at altitude h_1, is given by

$$p(h_1)=\frac{P_0 \Delta h}{2} A \frac{\beta(h_1)}{h^2} \exp\left[-2\int_0^{h_1} \alpha(h)\,\mathrm{d}h\right] \quad \ldots (1)$$

where

P_0 = transmitted power,
c = speed of light,
Δt = pulse width,
h = altitude,
E = optical efficiency of the transmitter and receiver optics,
A = Effective area of the receiving mirror,
$\beta(h_1)$ = volume backscatter coefficient at h_1
and
α = extinction coefficient.

$\beta(h_1)$ is given by

$$\beta(h_1)=n_a(h_1)\sigma_a+n_g(h_1)\,\sigma_g, \quad \ldots (2)$$

where σ_a and σ_g are the aerosol and molecular backscattering cross sections respectively and n_a and n_g are the number densities of aerosols and air molecules respectively. Similarly α is given by

$$\alpha(h)=n_a(h)\rho_a+n_g(h)\rho_g \quad \ldots (3)$$

where ρ_a and ρ_g are the extinction cross sections of aerosols and air molecules respectively. The lidar equation (equation 1) can be written in differential form, as

$$\frac{\mathrm{d}s}{\mathrm{d}h}=\frac{1}{\beta}\frac{\mathrm{d}\beta}{\mathrm{d}h}-2\alpha, \quad \ldots (4)$$

where

$s=\ln[p(h)h^2]$.

Eq. (2) contains two unknowns, namely α and β. Assuming a functional form of relationship between α and β the above equation can be solved[8,9] for α (or β) Using Fernald's method[9] of solving equation (2) with appropriate functional relationship between α and β, lidar observations of backscatter signal at Trivandrum have been analysed to obtain altitude profiles of aerosol extinction[7] Parameswaran *et al.*[10] carried out a comparison of aerosol extinction profiles obtained at Trivandrum and those obtained from SAGE II (Stratospheric Aerosol and Gas Experiment) satellite observations. The comparison showed a fairly good agreement with regard to both stratospheric and tropospheric aerosol extinction profiles. The comparison also revealed an increase in stratospheric aerosol extinction with decrease in latitude even within the tropical region. Further, the tropospheric aerosol extinction profiles revealed significant day to day as well longitudinal variabilities.

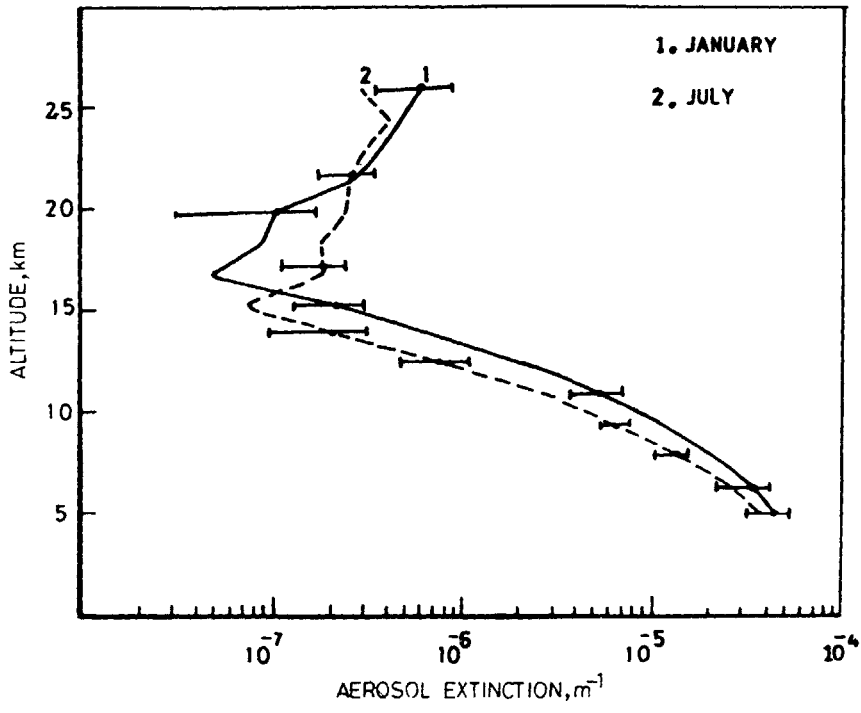

Fig 1 Monthly mean altitude profiles of aerosol extinction obtained from ruby lidar experiment at Trivandrum for (1) January 1987 and (2) July 1987

Tropospheric Aerosol Extinction

Parameswaran *et al.*[11] carried out a detailed study of the altitude profiles of tropospheric aerosol extinction and their temporal variations from lidar observations at Trivandrum over a period of about one and half years. They used the monthly mean profiles of aerosol extinction for this purpose. In Fig. 1 are shown the monthly mean profiles of aerosol extinction for January 1987 and July 1987 as typical examples. The lines parallel to the abscissa (in Fig. 1) show the standard deviations representing the day-to-day variations of the extinction. The altitude profiles show a smooth decrease with altitude up to about 17km (tropopause altitude) above which the extinction increases (in the stratosphere).

Making use of the monthly mean aerosol extinction profiles Parameswaran *et al.*[11]. estimated the (vertical) eddy diffusion coefficient at tropospheric altitudes. Considering steady conditions, the equilibrium aerosol number density in the middle and upper troposphere can be represented by the continuity equation as

$$\frac{\partial n}{\partial t} = q - an - bn^2 - \frac{\partial}{\partial h}(wn) + \frac{\partial}{\partial h}\left(D\frac{\partial n}{\partial h}\right) = 0, \qquad \ldots (5)$$

where n is the aerosol number density,

q is the aerosol production rate,
D is the eddy diffusion coefficient,
b is the coagulation coefficient,
a is the rate of loss by washout process, and
w_1 is the vertical velocity (gravitational sedimentation velocity).

In eq. (5), the aerosol production term, q is neglected as in the middle and upper tropospheres, the local production which is mainly by the gas to particle conversion process can be neglected in comparison with the other terms in the equation. In the aerosol size range of 0.02μm to 10μm which contributes to the backscatter/extinction at 694.3nm (ruby lidar operating wavelength) and at altitudes under consideration, the coagulation and gravitational sedimentation terms can be neglected. With these simplifications, the diffusion coefficient D can be obtained from eq. (5) as[11]

$$D \simeq \left(\frac{\partial n}{\partial h}\right)^{-1} \int_{h_1}^{h_2} an \, \mathrm{d}h \tag{6}$$

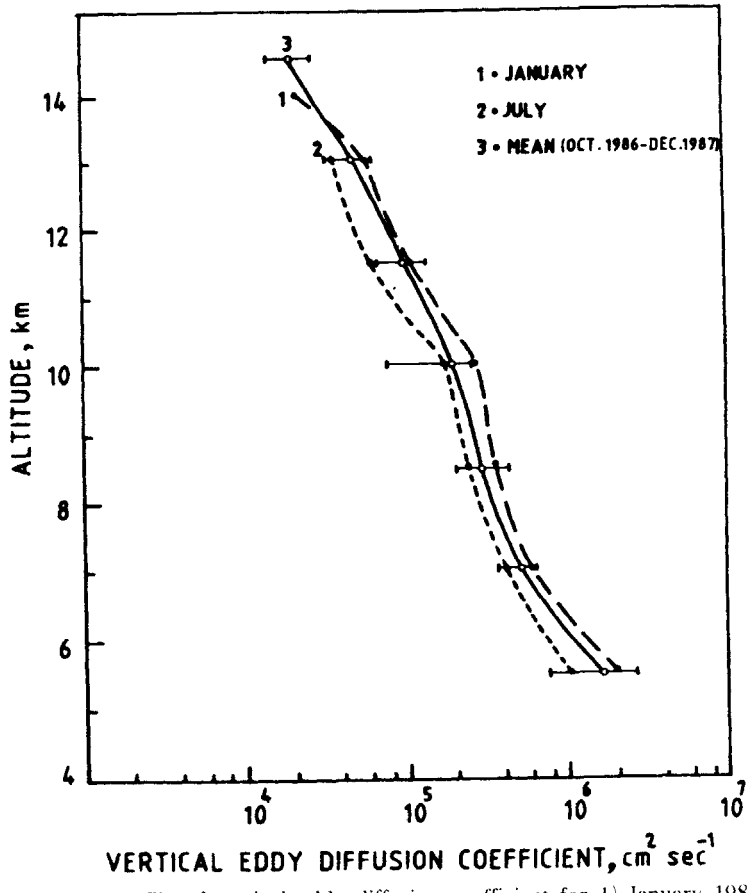

Fig 2 Mean altitude profile of vertical eddy diffusion coefficient for 1) January 1987, 2) July 1987 and 3) for the period October 1986 to December 1987

Adopting the model given by Turco *et al.*[12] for '*a*' Parameswaran *et al.*[11] estimated the vertical eddy diffusion coefficient '*D*' and their results are shown in Fig. 2 for the months January, 1987 and July 1987. The mean value of *D* (for the period of lidar observations from October 1986 to December 1987) is 4.8×10^5 cm^2 sec^{-1} at 5.5km altitude and decreases in nearly exponential manner with altitude. Parameswaran *et al.*[11] compared the diffusion coefficient profiles obtained by them with those obtained by earlier workers using data of Radon 222 gas and chemical releases and found good agreement. Thus, aerosol extinction or number density profiles can be used to estimate the vertical eddy diffusion coefficients in the middle and upper tropospheric regions.

Parameswaran *et al.*[11] studied the temporal variation of tropospheric aerosol extinction at different altitudes. Fig. 3 is a reproduction of their results. Shown in the same figure are also the integrated aerosol extinction from 4.8km to 16.8km and the monthly total rainfall at Trivandrum. The variations (with month) of aerosol extinction at altitudes ≤ 10.8km are quite similar whereas at higher altitudes, the variations are different from these especially in April-May,

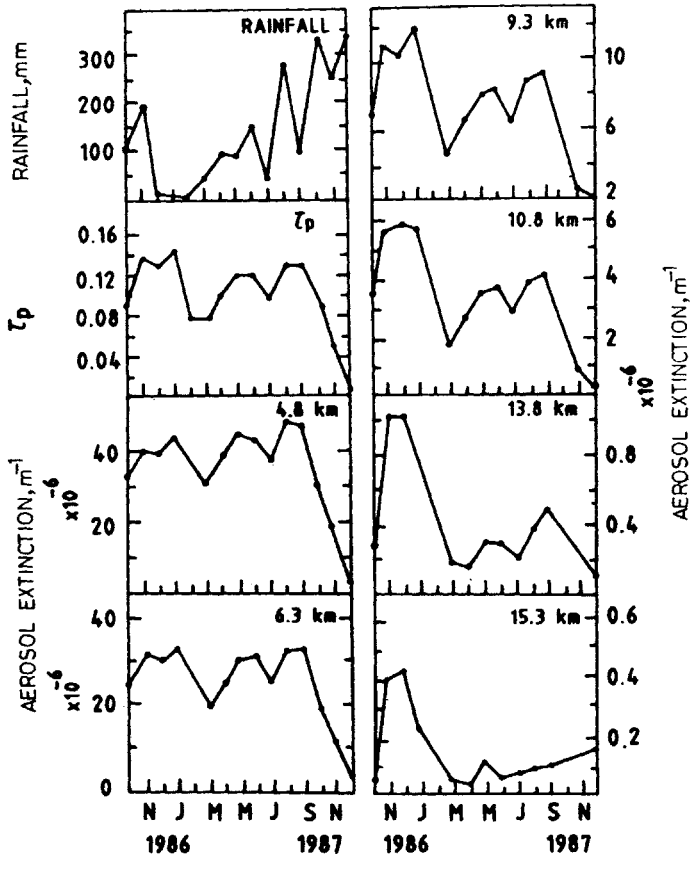

Fig 3 Temporal variation (*a*) of monthly mean aerosol extinction at different altitudes in the troposphere (*b*) τ_p, the total optical depth for the altitude range 3.8km to 16.8km and (*c*) monthly total rainfall

1987. There is a peak in the winter months of 1986-87 which is more prominent at higher altitudes. The sharp decrease in aerosol extinction at altitudes below 15.3km as well as in the integrated extinction during October-December 1987 can be attributed to strong wet removal of aerosols because of the heavy rainfall as indicated in the figure. This decrease (in extinction) is not seen at higher altitudes indicating that this loss process is not effective at these altitudes. The aerosol extinction peak during the summer/monsoon months can be attributed to *i*) an increase in production of aerosols from a possible increase of photochemical reactions due to volatile organic plant materials of plant origin, *ii*) an increase in tropospheric vertical mixing caused by high convective activity and *iii*) an increase in atmospheric water vapour content resulting in growth of aerosol particles. Further, at Trivandrum, strong surface winds during summer and monsoon months cause production of sea-spray aerosols due to sea-surface agitation[13]. These processes also could contribute to the peak in summer/monsoon months.

Stratospheric Aerosol Extinction

Stratospheric aerosols are mainly comprised of sulphuric acid-water solution droplets though ammonium sulphate is also present[14]. The sulphate particles are produced locally in the stratosphere mainly from precursor sulphur bearing vapours. Sulphur dioxide (SO_2) and carbonyl sulphide are the major precursor gases. SO_2 which is an important component of volcanic effluvia, is injected directly into the stratosphere during major volcanic eruptions. For instance, the eruption of Mt. Pinatubo volcano (Philippines) in June 1991 is estimated to have injected about 20 million tons of SO_2 into stratosphere which is about 3 times more than that due to the earlier volcanic eruption of El Chichon (Mexico) in March/April 1982. During volcanically quiescent periods, carbonyl sulphide (OCS) is the major precursor gas with carbon disulphide (CS_2) as a possible second source[16,17]. OCS originates mainly from biological and industrial sources and has very long tropospheric lifetime of several years[12]. In addition to OCS and CS_2, SO_2 from surface emission is transported to stratosphere during volcanically quiescent periods also. However, modelling studies[18,19] showed that OCS is the dominant sulphur source compared to CS_2 and SO_2 for stratospheric aerosols (during volcanically quiescent periods). The precursor gases are transported into stratosphere through eddy diffusion and direct injection which can occur during thunder cloud penetration, tropopause folding and vertical convection especially in the tropical zone. Horizontal advection subsequently distributes the injected material zonally and meridionally. OCS breaks up into sulphur and carbon monoxide by photodecomposition due to absorption in the extreme ultra violet (200-240nm) in the stratosphere. The sulphur atoms then react rapidly with molecular oxygen to form SO which on oxidation becomes SO_2. SO_2 is transformed into H_2SO_4 mainly through reactions involving OH radical. The H_2SO_4 thus produced and H_2O vapours nuclease by heterogeneous heteromolecular and homogeneous heteromolecular processes. In the former process, growth of pre-existing particles takes place due to condensation of H_2SO_4 and H_2O vapours. In the later process, new

particles are formed from gas phase consisting of H_2SO_4 and H_2O vapours and the newly formed particles further grow through condensation of these vapours. It is generally believed that the heterogeneous heteromolecular process is more efficient than the homogeneous heteromolecular process. However, recent modelling calculations in this regard[20] showed that at temperatures around $-75°C$ which are not uncommon in lower stratosphere, the homogeneous heteromolecular process can be a significant contributor to the overall nucleation process. Thus, stratospheric aerosols can be expected to show a significant dependence on temperature, Krishna Murthy *et al.*[21] investigated this aspect in detail using the stratospheric aerosol extinction profiles obtained from lidar observations at Trivandrum.

In Fig. 4 (from Krishna Murthy *et al.*[21]) is shown the variation of the monthly mean integrated stratospheric aerosol extinction and the monthly mean tropopause temperature. The variations of these two parameters are opposite to each other indicating a strong negative correlation between the two. The aerosol extinction at different stratospheric altitudes also showed similar monthly mean variations. Krishna Murthy *et al.* estimated the correlation coefficients between these parameters as shown in Table I. In this table, the correlation coefficients significant above $P = 0.05$ level[22] are indicated by asterisk.

The correlation (direct) of extinction at different altitudes with tropopause temperature is negative and significant whereas with ambient temperature, it is not significant though negative. A decrease in tropopause temperature is asso-

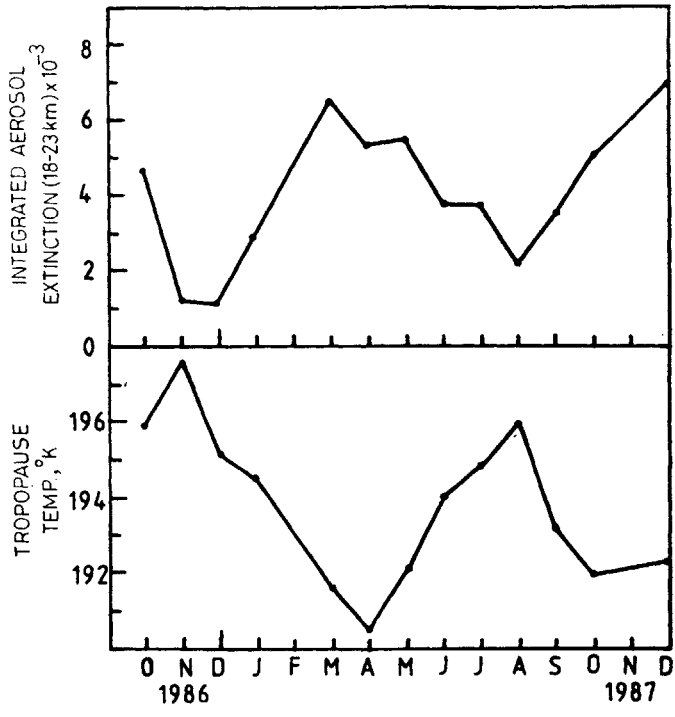

Fig 4 Temporal variations of monthly mean tropopause temperature and monthly mean integrated aerosol extinction (in Stratosphere)

Table I

Direct correlation coefficient (R) between aerosol extinction (α_a) at different stratospheric altitudes, ambient temperature (τ) tropopause temperature (τ_p), and partial correlation coefficients (r) between α_a and τ_p eliminating effect of τ and between α_a and τ eliminating effect of τ_p. Correlation coefficients significant at $p=0.05$ level are indicated with superscript of asterick

Altitude km	$R(\alpha_a, \tau)$	$R(\alpha_a, \tau_p)$	$R(\tau, \tau_p)$	$r(\alpha_a, \tau_p)$	$r(\alpha_a, \tau)$
18.3	−0.39	−0.65*	0.51	−0.57*	−0.09*
19.8	−0.44	−0.69*	0.40	−0.75*	−0.26*
21.3	−0.37	−0.72*	0.16	−0.72*	−0.36*
22.8	−0.17	−0.82*	−0.19	−0.88*	−0.57*

ciated with an increase in tropopause altitude which is indicative of stronger tropospheric convective activity[23]. This results in injection of significant tropospheric mass containing small size aerosol particles and aerosol precursor gases[24], OCS and SO_2. The injection of these constituents will lead to stratospheric aerosol nucleation and growth by condensation as discussed above and lower temperatures (ambient) are conducive for these processes. It is interesting to note that the partial correlation of aerosol extinction with ambient temperature eliminating the effect of tropopause temperature at 22.8km is significant whereas that at lower altitudes is not significant. These results clearly indicate that at lower stratospheric altitudes (<22km), aerosol extinction can mainly be attributed to direct particle injection across the tropopause whereas at higher altitudes, the stratospheric microphysical processes (heterogeneous heteromolecular and homogeneous heteromolecular processes) which are favoured by lower ambient temperatures become important. Further, Krishna Murthy *et al.*[21] showed that the observed increase in stratospheric extinction associated with lower temperature is consistent with the theoretical model calculations on stratospheric aerosols by Yue and Deepak[20]. These studies based on lidar observations at Trivandrum clearly brought out the effects of temperature on stratospheric aerosol extinction.

Studies on Total Aerosol Optical Depth

Total aerosol optical depth (τ_p) is very useful parameter in studies on temporal and spatial variations as well as radiative effects of aerosols. With a knowledge of τ_p and aerosol size distribution, the atmospheric path radiance and transmission coefficient can be obtained from approximate formulation of solution of radiative transfer equations assuming refractive indices[25]. As the chemical nature of different types of aerosols is known, refractive indices or at least the range of indices applicable can be inferred with a reasonable degree of confidence depending on the location. Study of aerosol total optical depth, size distribution, their temporal variations and long term trends would help in the understanding of the nature of aerosols and the relative contributions from natural and man-made sources. With this objective in view, study of total aerosol optical depths at different wavelengths in the range 400nm to 1025nm was in-

itiated in November 1985 at Trivandrum. A multi-wavelength solar radiometer (MWR) has been set up in November 1985 at Trivandrum for this purpose[26] Similar radiometers have been set up later under the Indian Middle Atmosphere Programme, at Mysore, Visakhapatnam, Jodhpur and New Delhi. The operation of these radiometers is being continued as part of the Geosphere-Biosphere Programme.

The radiometer operates at nine wavelengths, namely 400nm, 450nm, 500nm, 590nm, 700nm, 750nm, 800nm, 935nm and 1025nm with a bandwidth of 5nm. An additional wavelength 500nm is incorporated in September 1987. The direct solar flux is measured as a function of solar zenith angle. Using the standard Langley method, the total atmospheric optical depth (τ) is obtained from these measurements. τ consists of three components namely, *i*) molecular (Rayleigh) scattering, *ii*) gaseous absorption and *iii*) aerosol scattering and absorption. The first component is estimated by using the relevant expression for Rayleigh scattering and air densities[26]. The second component which is mainly due to ozone at some of the wavelengths (590nm) is estimated using the relevant absorption cross sections and densities of the corresponding

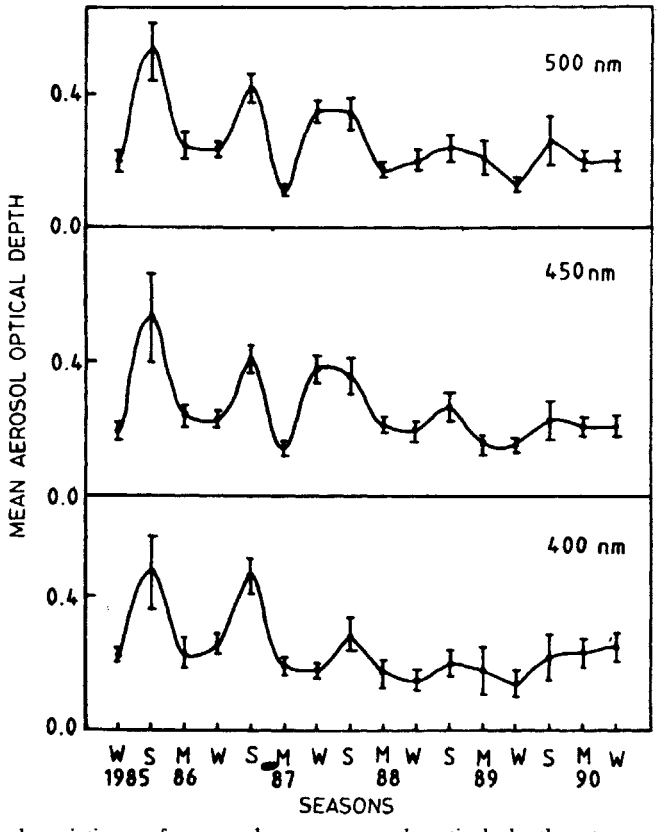

Fig 5 Temporal variations of seasonal mean aerosol optical depths at wavelengths 400nm, 450nm and 500nm. In the figure *W* indicates winter season comprising of December, January and February; *S* indicates summer season comprising of March, April and May months, *M* indicates monsoon season comprising of months from June to November

atmospheric constituents[26]. These two components thus estimated are then subtracted from τ to obtain total aerosol optical depth τ_p. The wavelength 935nm is used to estimate the total atmospheric water vapour content making using of the relatively strong water vapour absorption at this wavelength[13]. Altitude profiles of aerosol extinction obtained from lidar experiment[7] show that nearly 90% of the total aerosol extinction (optical depth) is contributed from the first 8 km and about 20% from the first 1km of the atmosphere from the ground. Thus, the total aerosol optical depths can mainly be attributed to aerosols in the altitude range 0-8km.

Figs 5, 6 and 7 show the variations of seasonal mean aerosol optical depths (at Trivandrum) at different wavelengths. It is readily seen from the figures that τ_p attains its maximum in summer and broad minimum in monsoon-winter seasons. However, the summer maximum becomes weaker and less pronounced in the later years (of the period of observations). Further, the seasonal variations appear to be wavelength dependent, with regard to their maximum to minimum ratio in an year. The standard errors are, in general, greater in summer than in the other two seasons, indicating greater day to day variability.

The seasonal variations of aerosol optical depths are to be understood in terms of the variations in different aerosol production, loss and transport processes. The main aerosol production/growth and loss processes are *i*) gas-to-particle conversion due to photochemical activity *ii*) particle growth by condensation of atmospheric water vapour *iii*) generation by wind and *iv*) rainout/washout (or wet removal processes). The first three processes of production/growth are likely to be prominent during local summer season. In addition to these, other aerosol sources and sinks of regional importance must also be considered. As Trivandrum is a coastal station, a significant aerosol input of marine origin can be expected. The strong westerly winds as well as the heavy rainfall associated with monsoon[27,28] are important in contributing to aerosol optical depth at this station. The south west monsoon setting-in during the first week of June at the coast of Trivandrum brings significant changes in tropospheric circulation earlier than its onset[29,30]. Strong surface westerly winds set-in from April onwards. These westerly winds gain strength with the advance of summer and results in considerable agitation of sea surface which manifest as sea surf and white caps. Considerable amount of marine aerosols is produced due to sea surf (and white caps) whose size spectrum and abundance depend upon the wind speed[31]. These marine aerosols are brought over to coastal land by the westerlies. As already pointed out, the wet removal process (rainout/washout) is a very important process of tropospheric aerosol removal and its strength is mainly determined by the rainfall. It should also be noted that surface wind (westerly monsoon winds) and rainfall which are effective in production and loss of aerosols respectively, themselves are associated with each other. In order to determine the effects of these two parameters on aerosol optical depths, correlation coefficients between these parameters are obtained. For this purpose the seasonal mean surface zonal wind speed (measured at a location near the MWR) and rainfall (of Trivandrum) are used. The correlation coefficients are shown in Fig. 8 for different wavelengths. Along with the direct correlation (r) between aerosol optical depth (r_{12}) with rainfall and wind (r_{13}),

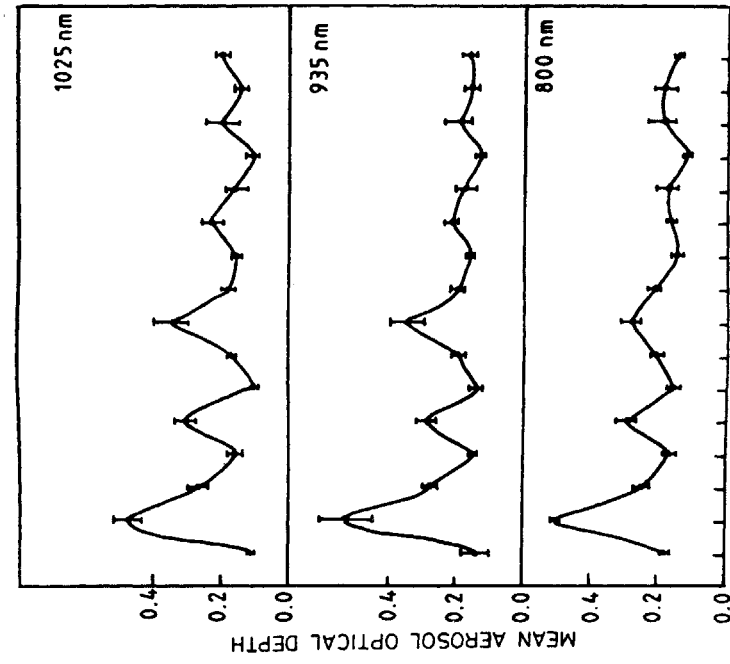

Fig 7 Same as Fig 5 except for 800nm, 935nm and 1025nm

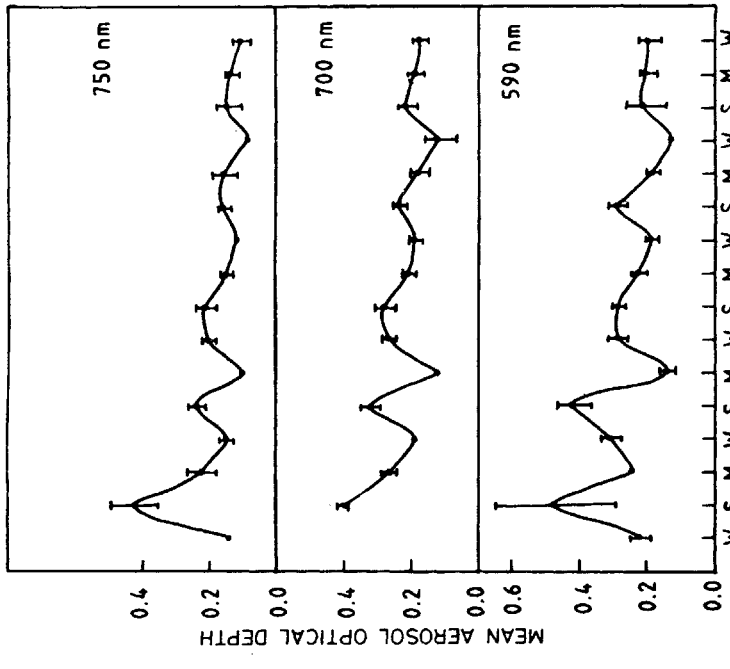

Fig 6 Same as Fig 5 except for 590nm, 700nm and 750nm

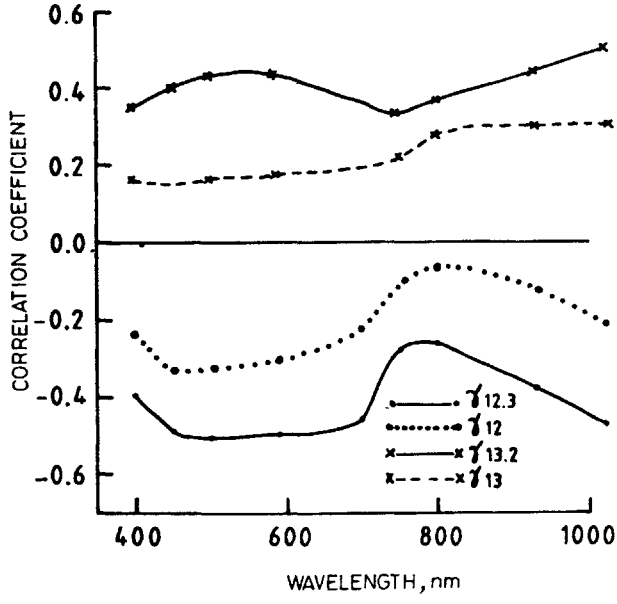

Fig 8 Correlation coefficients (r) as function of wavelength. In the figure suffixes (on r) 1, 2 and 3 represent seasonal mean optical depth, seasonal total rainfall and seasonal mean wind respectively

the partial correlation eliminating the effect of wind ($r_{12.3}$) and rainfall ($r_{13.2}$) are also shown in the figure. It is interesting to note that the partial correlations with wind and rainfall are positive and negative respectively which are, in general, significant and are greater than the direct correlation. This is because, as indicated earlier, wind and rainfall themselves are correlated (the correlation coefficient is 0.54 which is significant). This result (as shown in Fig. 8) indicates the effectiveness of wind and rainfall as production and loss agents of aerosols at the coastal station, Trivandrum. Thus the seasonal variations in aerosol optical depths can be attributed atleast partly, to these mechanisms. As there are various other production and loss mechanisms for aerosols as discussed earlier, observations spread over a longer period would certainly help to delineate the effects of these sources/sinks in a more unambiguous manner.

Aerosol Columnar Size Distributions

Aerosol optical depth $\tau_p(\lambda)$ can be written as

$$\tau_p(\lambda) = \int_{r_1}^{r_2} \pi r^2 \, Q_{\text{ext}}(r, m, \lambda) n_c(r) \mathrm{d}r,$$

where

r is radius of the aerosol particle (assumed spherical),
Q_{ext} is the Mie extinction efficiency factor,
m is the complex refractive index,
λ is the wavelengths at which τ_p is obtained,
and

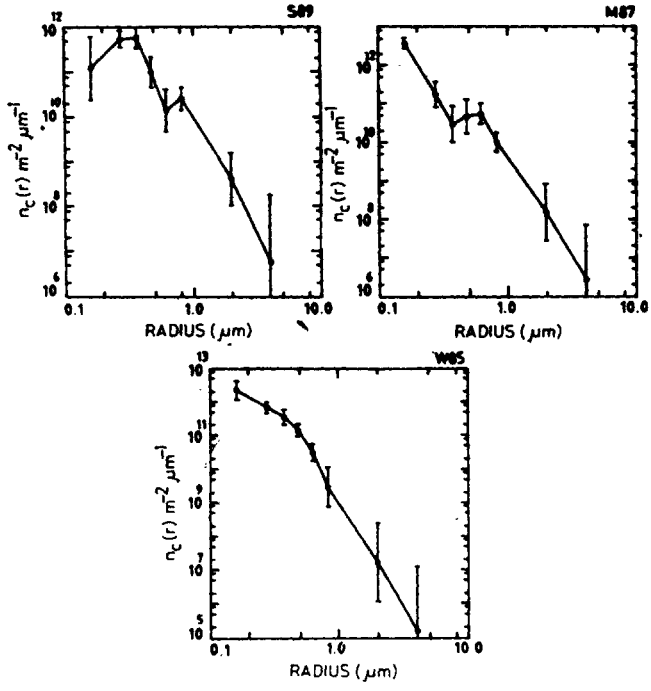

Fig 9 Aerosol columnar size distributions for summer 1989 (S 89), Monsoon 1987 (M 87) and winter 1985 (W85)

$n_c(r)$ is the total atmospheric aerosol content at radius r per unit radius interval.

By inverting the above equation, the columnar aerosol size distribution $n_c(r)dr$ can be obtained. This equation is similar to the Fredholm integral equation of the first kind. Methods of inverting the above equation for obtaining $n_c(r)dr$ are dealt with in literature[32,33]. Krishna Moorthy *et al.*[13] adopting the method of King *et al.*[32] derived the columnar aerosol size distributions from $\tau_p(\lambda)$ data at Trivandrum.

The columnar aerosol size distributions have been derived using the seasonal mean aerosol optical depth data at Trivandrum. In Fig. 9 are shown typical examples of the size distributions for the three seasons. The main features of the seasonal characteristics of the size distributions are the following:-

i) The size distributions are bimodal type in all the summer seasons (from November 1985 to February 1990) with the secondary mode at aerosol radius of ~ 1 μm.

ii) The winter size distributions are mainly unimodal or inverse power law type.

iii) The monsoon size distributions show variability in functional form in different years. They are either bimodal or unimodal or inverse power law type.

The appearance of a secondary mode consistently in summer is indicative of an additional source of aerosols. It is pointed out earlier that in summer

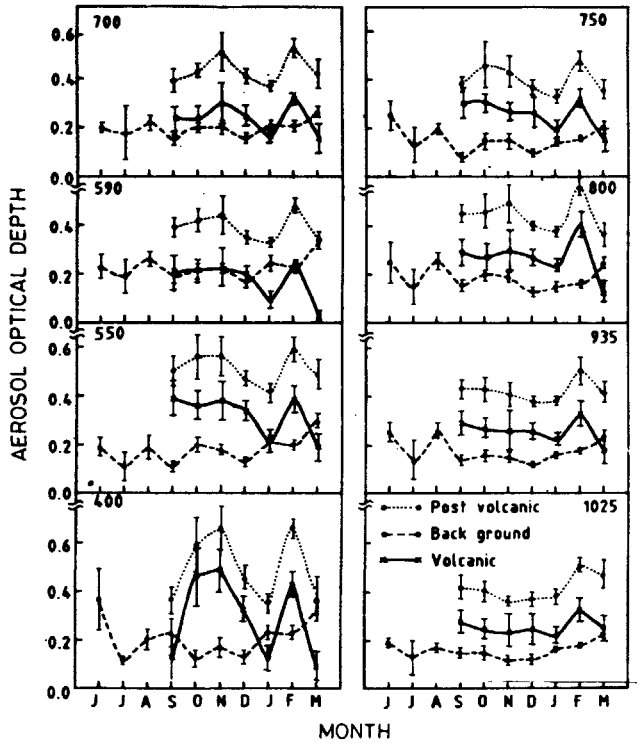

Fig 10 Temporal variations of monthly mean optical depths corresponding to post-volcanic, background and volcanic conditions

season, strong westerly wind is presently giving rise to sea surface agitation and consequent production of sea spray aerosols. The sea spray aerosols produced are known to be of size $>0.5\mu$m. The secondary mode appearing in summer season size distribution can be attributed mainly to this additional source of aerosols. In the monsoon, in addition to the production of sea spray aerosols, the loss process due to wet removal would be quite significant owing to heavy rainfall during this season. Thus, the nature of monsoon size distribution would depend upon the relative effectiveness of these strong production (sea spray aerosols) and loss (wet removal) processes. Thus, the observed variability in the monsoon size distribution for different years may be attributed to the variability in the relative strengths of these processes. The winter season is characterized by weak surface winds and insignificant rainfall. The photochemical processes leading to gas-to-particle conversion also become weak. Thus the winter aerosols can be considered to represent the background condition. When the main production and loss processes are weak, coagulation and gravitational sedimentation will be the dominant processes affecting the size distributions. Coagulation in the small particle range and gravitational sedimentation in the large particle range would result in a unimodal distribution which is observed, in general, in winter.

The total volume V_L of aersols is estimated by

$$V_L = \int_{r_1}^{r_2} r^3 n_c(r)\, dr \qquad \ldots (8)$$

It is found that partial correlation of V_L with wind eliminating the effect of rainfall is significantly positive and that with rainfall eliminating the effect of wind is significantly negative. This result further confirms the effect of wind and rainfall on aerosols discussed earlier in terms of aerosols optical depths.

Effect of Mt. Pinatubo Volcanic Eruption on Aerosol Optical Depths

Mt. Pinatubo Volcano (15°N, 120°E) situated in Philippines erupted in June, 1991, injecting large quantities of SO_2 gas and ash into the atmosphere. It was estimated that the ejected mass of SO_2 was about 20 million tones[15]. This quantity of SO_2 converted to sulphuric acid aerosols in stratosphere, resulted in substantial (additional) aerosol loading.

Using the Multiwavelength radiometer at Trivandrum, the effect of the volcanic aerosol loading on aerosol optical depths has been investigated. Fig. 10 shows the monthly mean aerosol optical depths at the different wavelengths due to post volcanic, background and volcanic aerosols for different months[34]. The background aerosol optical depths are obtained by averaging the aerosol optical depths for the same months in different years and the volcanic aerosol optical depths are obtained by subtracting the background aerosol optical depths from the post volcanic optical depths for different months.

It can be clearly seen that there is substantial enhancement in the aerosol optical depth following the volcanic eruption. The enhancement showed temporal variations with peaks in October-November 1991 and February 1992 with the strengths of these peaks varying with wavelengths. The size distribution of the volcanic aerosols have been estimated using this optical depth data. It is found that the size distributions generally exhibit a strong peak around $0.75\mu m$ and that the temporal changes in the size distribution occurred mainly in the small particle range. This can be attributed to the conversion of the small particles to larger sizes by coagulation. The volcanic aerosol mass loading (columnar) is found to be ~ 145 milli grams/m^2.

References

1 A Robock *Geofis Int* **23** (1984) 403
2 M C McCracken and F M Luther *Geofis Int* **23** (1984) 385
3 R K R Vupputuri and J P Blanchet *Geofis Int* **23** (1984) 433
4 K Labitzke, B Naujokat and M P McCormick *Geophys Res Lett* **10** (1983) 24
5 K Labitzke and M P McCormick *Geophys Res Lett* **19** (1992) 207
6 D J Hofmann *Rev Geophys* **25** (1987) 743
7 K Parameswaran, K O Rose, M Satyanarayana and B V Krishna Murthy *Indian J Radio & Space Phys* **18** (1989) 202
8 J D Klett *Appl Opt* **20** (1981) 211
9 F G Fernald *Appl Opt* **23** (1984) 652

10 K Parameswaran, K O Rose, B V Krishna Murthy, M T Osborn and L R Mcmaster *J geophys Res* **96** (1991) 10861
11 K Parameswaran, B V Krishna Murthy, K O Rose and M Satyanarayana *Ann Geophys* **11** (1993) 61
12 R P Turco, P Hamill, O B Toon, R C Whitten and C S Kiang *J atmos Sci* **36** (1979) 699
13 K Krishna Moorthy, P R Nair and B V Krishna Murthy *J appl Meteorol* **30** (1991) 844
14 P Hamill, O B Toon and C S Kiang *J atmos Sci* **34** (1977) 1104
15 G T S Bluth, S D Doiron, C C Schnetzler, A J Krueger and L S Walter *Geophys Res Lett* **19** (1992) 151
16 N D Sze and M K W Ko *Atmos Environ* **14** (1980) 1223
17 P J Crutzen *Geophys Res Lett* **3** (1976) 73
18 R P Turco, R C Whitten, O B Toon, J B Pollock and P Hamill *Nature* **283** (1980) 283
19 R P Turco, O B Toon, R C Whitten, E C Y Inn and P Hamill *J Geophys* **86** (1981) 1129
20 G K Yue and A Deepak *Appl Opt* **20** (1981) 3669
21 B V Krishna Murthy, K Parameswaran, K O Rose and M Satyanarayana *J atmos Terr Phys* **55** (1993) 809
22 R A Fisher *Statistical Methods for Research Works* Oliver and Boyd, Edinburgh (1970)
23 B V Krishna Murthy, K Parameswaran and K O Rose *J atmos Sci* **43** (1986) 914
24 R P Turco, R C Whitten and O B Toon *Rev Geophys Space Phys* **20** (1982) 233
25 B C Forster *Int J Remote Sensing* **5** (1984) 799
26 K Krishna Moorthy, P R Nair and B V Krishna Murthy *Indian J Radio Space Phys* **18** (1989) 194
27 Y P Rao Southwest Monsoon *Meteorol Monograph Synoptic Meteorology*, No 1/1976, India Meteorology Department, New Delhi (1976)
28 P K Das *Monsoons*, WMO-No 613 (1986)
29 V Narayanan *Indian J Meteorol Geophys* **18** (1967) 497
30 N S Nair and V Narayanan *Monsoon* **31** (1980) 409
31 C E Junge *Air Chemistry and Radioactivity* Academic Press, New York (1963)
32 M D King, D M Byrne, B M Herman and J A Reagan *J atmos Sci* **35** (1978) 2153
33 M D King *J atmos Sci* **39** (1982) 1356
34 B V Krishna Murthy, K Krishna Moorthy and P R Nair *Geophys Res Lett* (1993)